

LFC of Smart Open Market Power System Using TSMC-DDC with Communication Delay

K.Kranti Kumar¹, T. Anil Kumar²

¹School of Engineering, Anurag University

²School of Engineering, Anurag University

E-mail: ¹kranthi.dee@gmail.com, ²thalluru.anil@gmail.com

ARTICLE INFO

ABSTRACT

Received: 24 Dec 2024

Revised: 12 Feb 2025

Accepted: 26 Feb 2025

In restructured power system Load Frequency Control (LFC) is a serious problem due to sudden fluctuation of load demand among DISCOS within and outside of the Control Area. The Dynamic Demand Control (DDC) is a strategy that improves LFC by changing the instantaneous power demand to match the generation, thus providing a more flexible and intuitive system. DDCs, which enhance the frequency of power systems mainly for renewable energy integrated power systems. This paper submits a contribution LFC, including DDC, with the inherent communication latency in smart grid structures. A Terminal Order Sliding Mode Controller (TSMC)-DDC was proposed with communication delay to address the LFC of three-area deregulated power systems integrated with renewable energy and EV integrated power systems. The performance of the TSMC-DDC was tested on an open market three area renewable energy and EV Integrated power system.

Keywords: Load Frequency Control (LFC), Dynamic Demand Control (DDC), Deregulated Power System (DPS), Independent System Operator (ISO), Terminal Order Sliding Mode Control (TSMC), Control Area(CA).

INTRODUCTION

In power system frequency deviation occurs when generation not meeting the load demand[1]. In open market renewable and EV integrated power system due to intermittency of renewable energies and sudden fluctuation of load demand due to incentives offered by the DISCOMS causes load frequency control problem of power system[2]. The scheduled system frequency maintained by effectively distributing the load among MW output of generators and ensuring adherence to tie-line power interchange schedules[3-4]. The problem of frequency regulation has long been a major challenge in the operation of electric power systems. Deviations from normal frequency conditions can severely affect system performance and reliability. The primary objectives of LFC in power systems is to maintain the frequency nominal value and to ensure that power exchanges with neighbouring control areas adhere to scheduled values. These objectives are essential for ensuring stability and preventing operational failures in interconnected system [5].

The LFC is more complicated with renewable energy integration into the power grid due to their inherent variability and uncertainty [6]. The transition from a vertically integrated utility model to a more competitive framework in the power sector has led to remarkable changes in both planning and operation. In deregulation the introduction of smart grid technologies has revised traditional power systems to intensify customer benefits by providing lower tariffs, more choices, and better service quality [7]. In the open market power system allows for greater market competition and efficiency, although GENCOs focus on electricity generation and not participate in LFC systems directly. GENCOs and DISCOMS engage in many bilateral contracts, permitting them to negotiate terms that best meet their operational and financial needs.

This shift towards deregulation not only promotes competitive pricing but also improves reliability and quality of service, ultimately benefiting consumers through more responsive and flexible electricity supply systems. The integration of smart grid technologies further facilitates real-time data management and improves grid resilience, marking a significant advancement in how electricity is generated, transmitted, and consumed [8]. In a deregulated electricity market, ISO plays a key role in ensuring the stability, reliability, and efficiency of the power grid. In a

smart grid bidirectional information flow where consumer interact with DISCOMS lead to consumer satisfaction [9].

The Dynamic Demand Control (DDC) is indeed an exciting development in electricity demand management, especially with the integration of variable RES by enabling real-time adjustments to non-essential loads—like refrigerators, air conditioners, and water heaters—DDC can enhance grid stability and balance supply and demand more effectively [10].

A fuzzy-PI-based supervisory controller is propounded to facilitate the coordination between the demand response and LFC, adjusting responsive generators according to the regulation provided by the regional demand response (RDR). This coordinator effectively addresses system uncertainties, and the time delay effects associated with the RDR scheme [11]. The frequency control strategy for demand response (DR) in a multi-area power system is carefully developed to rapidly stabilize the frequency across various regions by incorporating the tie-line power as an additional input signal for DR, this method improves the overall effectiveness of frequency control [12].

Furthermore, delay margins for LFC with DDC were assessed through a trial-and-error simulation method, which revealed several stability regions. This indicates that substantial delays could result in the re-stabilization of the LFC system [13]. The impact of an intelligent DR control loop was investigated by taking communication delays into account in a single-area thermal power system that incorporates a wind power system [14].

Communication delays can reduce the response of control systems to changes in frequency or load. This delay may lead to insufficient or excessive adjustments in generation or demand, resulting in frequency deviations. If the system cannot respond rapidly to these disturbances, oscillations may occur, leading to system instability [15]. In DDC, where load-side resources like smart appliances and electric vehicles are adapted based on system requirements, communication delays can obstruct timely coordination between supply and load adjustments. An open communication in power system allows sustaining the progressively decentralized control process in an open market deregulated power system. Open communication systems are preferred over dedicated communication networks for the present LFC scheme owing to their economical and flexibility advantages. Time delays may emerge through an open communication network due to a backlash (or a dead zone) from an external environment [16].

In general, the loads on the customer side are perpetually changing with respect to time and develop a power discrepancy with the generation, this power discrepancy causes certain oscillations in the operation of the power system, and it causes a certain frequency deviation from the scheduled frequency [17]. The PID controllers are commonly used in LFC due to their simplicity and effectiveness. However, they often result in long settling times and significant overshoots in the frequency transient response, and they lack robustness against disturbances and uncertainties [18]. In contrast, sliding mode control (SMC) is a robust controller that does not depend on an accurate system model, making it effective for managing system dynamics under external disturbances and internal uncertainties. However, standard SMC is associated with chattering issues, which can cause undesirable oscillations, increased actuator wear, and degraded system performance [19]. In this paper the modelling of restructured power system with DDC and modelling of the Terminal Order Sliding Mode Controller discussed in section II&III respectively. The discussion on simulation results and conclusions are presented in IV &V respectively.

MODELLING OF DPS WITH DDC

The LFC model of multi-area in a deregulated structure shown in fig-1[20], in which every GENCO can contract with DISCOs belonging to the same or other control areas. These bilateral contracts can be represented using an augmented generation participation matrix (AGPM) [21]. The AGPM shows each Genco's participation factor in the control areas, and each control area is bounded by a Disco. In AGPM [5], the row gives the number of the Genco's, and columns represent the contract power of the control areas.

$$AGPM = \begin{bmatrix} gpf_{11} & \dots & gpf_{1(m-1)} & gpf_{1m} \\ gpf_{21} & \dots & gpf_{2(m-1)} & gpf_{2m} \\ \vdots & \vdots & \vdots & \vdots \\ gpf_{(n-1)1} & \dots & gpf_{(n-1)(m-1)} & gpf_{(n-1)m} \\ gpf_{n1} & \dots & gpf_{n(m-1)} & gpf_{nm} \end{bmatrix} \quad (1)$$

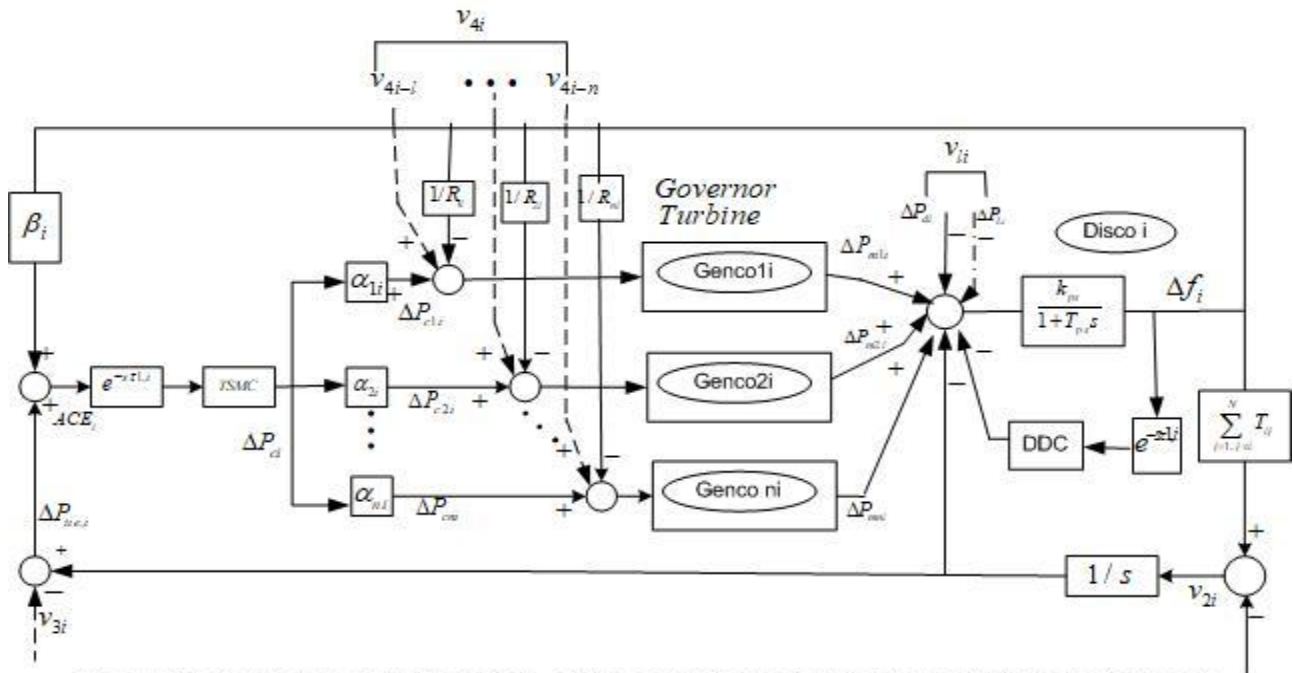


Fig-1. Block diagram representation of the control area i under deregulated environment

The gpf_{mn} denote generation participation factor indicates the contribution of each Generation Company (GENCO) toward fulfilling the total load demand specified by the Distribution Company (DISCO). Each column's entries sum to one, ensuring that the combined generation from all GENCOs aligns precisely with the load demand established by DISCO.

$$\sum_{n=1}^n gpf_{ni} = 1 \quad (2)$$

The v_{ii} is the sum of area load disturbance (ΔP_{di}) and local contracted demand (ΔP_{Li}).

$$v_{ii} = \Delta P_{di} + \Delta P_{Li} \quad (3)$$

Whereas

$$v_{2i} = \sum_{j=1, j \neq i}^N T_{ij} \Delta f_j \quad (4)$$

The v_{2i} represents the combine outcome of each area with other areas.

Where T_{ij} is tie-line synchronizing coefficient, Δf_j is the frequency drift in area j.

This is the scheduled tie-line power change.

$$v_{3i} = \sum_{j=1, j \neq i}^N \left(\sum_{k=1}^n gpf_{kj} \right) \Delta p_{Lj} - \sum_{k=1}^n \left(\sum_{j=1, j \neq i}^N gpf_{kj} \right) \Delta p_{Lj} \tag{5}$$

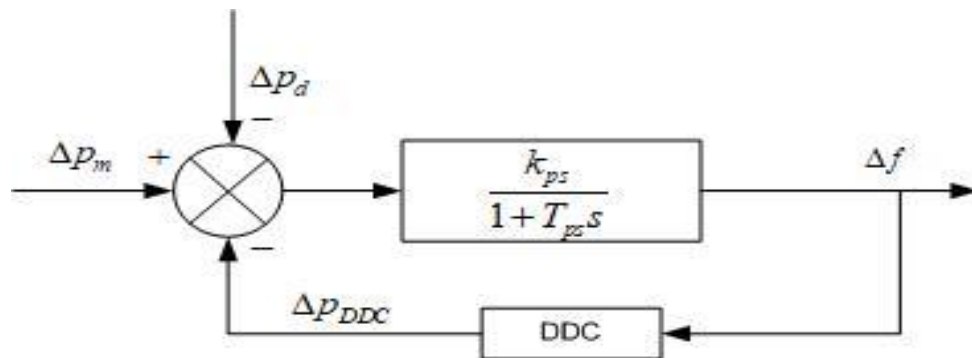


Fig 2 . Conventionalized model of the deregulated LFC with DDC

The v_{4i} is the contracted demand of other Discos from Genco’s of area i

$$v_{4i-n} = [v_{4i-1} v_{4i-2} \dots v_{4i-n}] \tag{6}$$

$$v_{4i-n} = \sum_{j=1}^N gpf_{nj} \Delta p_{Lj} \tag{7}$$

The mechanical power change ($\Delta p_{m,i-n}$) of every Genco can be found as given by

$$\Delta p_{m,i-n} = v_{4i-n} + \alpha_{ni} \sum_{j=1}^{m_i} \Delta p_{ULj-i}, \quad n=1,2,\dots,n_i \tag{8}$$

Where α_{ni} represents the area control error, which plays a major role when un-contracted demands exist and Δp_{ULj-i} is un-contracted demand of Genco j in area ‘i’.

A. DDC model for LFC

The loads which are convert electricity into heating and cooling can be utilized for DDC. These loads, which automatically adjust their operation based on temperature settings, can be managed through DDC to enhance system efficiency, balance load, and improve grid stability in real-time [22]. In this paper air conditioner are participating in the DDC in which the adjustable loads participate by changing their usage of electricity pattern depending on the changes in the load frequency of a renewable energy integrated power system.

The deviation in power due to thermostatic loading

$$\Delta P_{\dot{\alpha},i} = \Delta P_{LC,i} + D_{ac,i} \Delta \omega \tag{9}$$

The change in load is ΔP_{LC} and $D_{ac,i}$ is the reheat coefficient.

The change in air conditioner load is given in the below equation

$$\Delta P_{LC,i} = (m_i c_{p,i} \Delta T_{st,i}) / EER \tag{10}$$

$m_i, c_{p,i}, \Delta T_{st,j}$ are the mass of air flow, air specific gravity and $\Delta T_{st,j}$ is the smart thermostat’s set point respectively.

The temperature set point $\Delta T_{st,i}$ of a smart thermostat is given as with the change in frequency (Δf_i) of the i th control area.

$$\Delta T_{st,i} = k \int \alpha \Delta f_i dt \tag{11}$$

The smart thermostat’s gain factor is labelled as k and is considered as 10; α is taken as 0.5 Rs/Hz.

The temperature set point of the thermostat between 24°C to 29°C.

The air conditioner load model is represented as follows:

$$\begin{aligned} \Delta P_{dck,i} &= (m_i c_p, i k \int 0.5 \Delta f_i dt) / EER + D_{\alpha,i} 2 \Pi \Delta f \\ &= 0.5 k_i \int \Delta f_i dt + 2 \Pi D_{\alpha,i} \Delta f \end{aligned} \tag{12}$$

where $k_i = \frac{m_i c_p, i k}{EER}$

TERMINAL ORDER SLIDING MODE CONTROLLER (TSMC) FOR OPEN MARKET SMART RESTUCTURED POWER SYSTEM FOR LFC

A SMC is a robust controller category that provides insensitivity to variations caused by load disturbances, output variations from non-conventional sources and system parameter deviations. SMC uses conventional linear sliding surfaces, which ensure asymptotic stability. However, one major drawback of SMC is the chattering effect, which must be carefully addressed when applied to load frequency control systems. To reduce these issues, an alternate development in the field is the time sliding mode controller (TSMC) [23].

The design of a TSMC involves two key steps: (a) defining the switching surface and (b) developing the control law. The sliding surface, a hyper surface within the system's state space, is designed to drive the system states to a desired manifold in finite time. The primary challenge lies in guiding trajectories to the sliding surface and ensuring that they remain confined to it. The sliding mode control law addresses this by driving any initial trajectory to the sliding surface within a finite time and maintaining it on the surface after that [24].

The dynamic nonlinear power system characterized in state-space [25].

$$\dot{x}_n = f(x) + d(x) + b(x)u \tag{13}$$

$f(x)$ is a system state vector, $d(x)$ represents the system uncertainties and x is a state vector.

A. Design of switching surface

In sliding manifold of the TSMC can be designed as

$$s = x_n + c_{n-1} \operatorname{sgn}(x_{n-1}) |x_{n-1}|^{\alpha_{n-1}} + \dots + c_1 \operatorname{sgn}(x_1) |x_1|^{\alpha_1} \tag{14}$$

Where c_i and α_i ($i=1,2,\dots, n-1$) are two group of parameters, which need to be designed.

$$\alpha_i = \frac{\alpha_i \alpha_{i+1}}{2\alpha_{i+1} - \alpha_i} \quad i = 1, 2, \dots, n-1 \tag{15}$$

$$\alpha_n = 1, \alpha_{n-1} = \alpha, \alpha \in (1 - \varepsilon, 1), \varepsilon \in (0, 1)$$

The condition given below for existence of sliding mode (Edwards & Spurgeon 1998):

$$\frac{1}{2} \frac{d}{dt} s^2 < -\eta |s| \tag{16}$$

Where $\eta > 0$ is a constant.

Once the ideal sliding-mode $s=0$ is developed, system (13) exhibits the same behaviour, specifically:

$$x_n = -c_{n-1} \operatorname{sgn}(x_{n-1}) |x_{n-1}|^{\alpha_{n-1}} - \dots - c_1 \operatorname{sgn}(x_1) |x_1|^{\alpha_1} \tag{17}$$

The above equation can also be written:

$$\dot{x}_{n-1} = -c_{n-1} \operatorname{sgn}(x_{n-1}) |x_{n-1}|^{\alpha_{n-1}} - \dots - c_1 \operatorname{sgn}(x_1) |x_1|^{\alpha_1} \tag{18}$$

B. Controller Design:

The design of the TSMC control law given as

$$u = b^{-1}(x)(-f(x) + \operatorname{sat}(u_f, u_s) - k \operatorname{sgn}(s)) \tag{19}$$

With

$$u_f = -c_{n-1} \alpha_{n-1} x_{n-1}^{\alpha_{n-1}-1} x_n - \dots - c_1 \alpha_1 x_1^{\alpha_1-1} x_2 \tag{20}$$

Where $\eta > 0$ is the control gain and $\operatorname{sgn}(\cdot)$ is the function. The controller in (17) ensures the system (13) satisfies sufficient condition for the sliding mode’s existence.

IV . SIMULATION RESULTS AND DISCUSSIONS

The multi area EV and renewable integrated three area open market power system with two GENCOs and two DISCOMs in each area with DDC shown in fig-4. The TSMC is introduced in each CA with a system transportation lag 0.1 sec of each control area.

The total demand for DISCOs is

$$\Delta p_M = \sum_j gpf_j \Delta p_{Lj} \tag{21}$$

For the three-area case

$$\begin{bmatrix} \Delta p_{M1} \\ \Delta p_{M2} \\ \Delta p_{M3} \\ \Delta p_{M4} \\ \Delta p_{M5} \\ \Delta p_{M6} \end{bmatrix} = \begin{bmatrix} gpf_{11} & gpf_{12} & gpf_{13} & gpf_{14} & gpf_{15} & gpf_{16} \\ gpf_{21} & gpf_{22} & gpf_{23} & gpf_{24} & gpf_{25} & gpf_{26} \\ gpf_{31} & gpf_{32} & gpf_{33} & gpf_{34} & gpf_{35} & gpf_{36} \\ gpf_{41} & gpf_{42} & gpf_{43} & gpf_{44} & gpf_{45} & gpf_{46} \\ gpf_{51} & gpf_{52} & gpf_{53} & gpf_{54} & gpf_{55} & gpf_{56} \\ gpf_{61} & gpf_{62} & gpf_{63} & gpf_{64} & gpf_{65} & gpf_{66} \end{bmatrix} \begin{bmatrix} \Delta p_{L1} \\ \Delta p_{L2} \\ \Delta p_{L3} \\ \Delta p_{L4} \\ \Delta p_{L5} \\ \Delta p_{L6} \end{bmatrix} \tag{22}$$

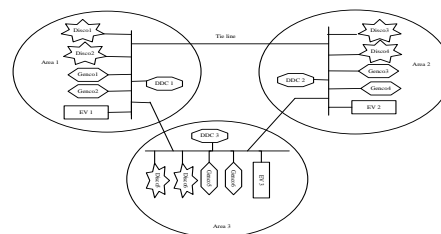


Fig. 3. Configuration of Three-area decentralized power system

A. Bilateral Based Transactions:

In these transactions, the DISCOs transacting power from other CA or with in the CA. Considering all DISCOs in the three areas are experiencing a step load disturbance of 0.1 p.u. The steady state output power of each generator is determined by theoretically for the enhanced load demand. The AGPM is considered for bilateral transactions.

$$AGPM = \begin{bmatrix} 0.25 & 0 & 0.25 & 0 & 0.5 & 0 \\ 0.5 & 0.25 & 0 & 0.25 & 0 & 0 \\ 0 & 0.5 & 0.25 & 0 & 0 & 0 \\ 0.25 & 0 & 0.5 & 0.75 & 0 & 0 \\ 0 & 0.25 & 0 & 0 & 0.5 & 0 \\ 0 & 0 & 0 & 0 & 0 & 1 \end{bmatrix} \tag{23}$$

From equation (22) , we can write

$$\Delta P_{M1} = gpf_{11}\Delta P_{L1} + gpf_{12}\Delta P_{L2} + gpf_{13}\Delta P_{L3} + gpf_{14}\Delta P_{L4} + gpf_{15}\Delta P_{L5} + gpf_{16}\Delta P_{L6}$$

$$= 0.25 \times 0.1 + 0 \times 0.1 + 0.25 \times 0.1 + 0 \times 0.1 + 0.5 \times 0.1 + 0 \times 0.1$$

$$\Delta P_{M1} = 0.1 \text{ puMW}$$

in the same way

$$\Delta P_{M2} = 0.1 \text{ puMW}; \Delta P_{M3} = 0.075 \text{ puMW}; \Delta P_{M4} = 0.15 \text{ puMW}; \Delta P_{M5} = 0.075 \text{ puMW};$$

$$\Delta P_{M6} = 0.1 \text{ puMW}$$

An analysis of the frequency change across the three areas indicates that, as shown in Figures 1 (a), (b), and (c), the frequency in each area stabilizes to zero in less than 21 seconds when using TSMC. The tie line power deviations are determined by using equations (24) (25) & (26).

$$\Delta P_{tie12} = \{ \text{Demand of Discos in area -2 from GENCOs in area -1} \} - \{ \text{Demand of DISCO area-1 from GENCOs in area -2} \} \quad [26][27]$$

$$\Delta P_{tie12} = [gpf_{13}\Delta P_{L3} + gpf_{23}\Delta P_{L3} + gpf_{14}\Delta P_{L4} + gpf_{24}\Delta P_{L4} + gpf_{31}\Delta P_{L1} + gpf_{41}\Delta P_{L1} + gpf_{32}\Delta P_{L2} + gpf_{42}\Delta P_{L2}] \quad (24)$$

$$\Delta P_{tie12} = [0.25 \times 0.1 + 0 \times 0.1 + 0 \times 0.1 + 0.25 \times 0.1] - [0 \times 0.1 + 0.25 \times 0.1 + 0.5 \times 0.1 + 0 \times 0.1] = -0.025 \text{ puMW}$$

$$\Delta P_{tie23} = \{ \text{Demand of Discos in area -3 from Gencos in area -2} \} - \{ \text{Demand of Discos in area-2 from Gencos in area -3} \}$$

$$\Delta P_{tie23} = [gpf_{35}\Delta P_{L5} + gpf_{36}\Delta P_{L6} + gpf_{45}\Delta P_{L5} + gpf_{46}\Delta P_{L6}] - [gpf_{53}\Delta P_{L3} + gpf_{54}\Delta P_{L4} + gpf_{63}\Delta P_{L3} + gpf_{64}\Delta P_{L4}] \quad (25)$$

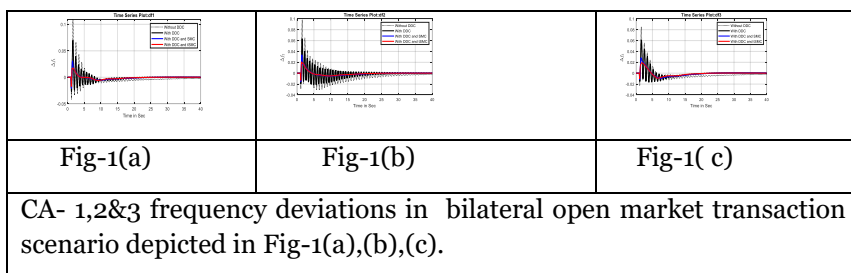
$$\Delta P_{tie23} = [0 \times 0.1 + 0 \times 0.1 + 0 \times 0.1 + 0 \times 0.1] - [0 \times 0.1 + 0 \times 0.1 + 0 \times 0.1 + 0 \times 0.1] = 0 \text{ puMW}$$

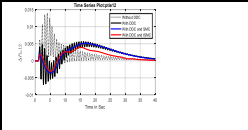
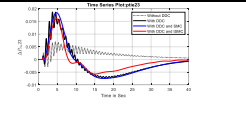
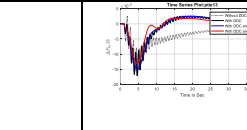
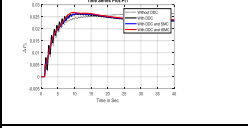
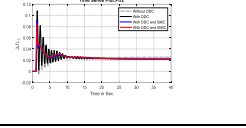
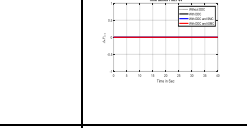
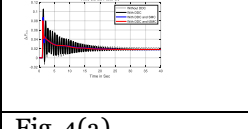
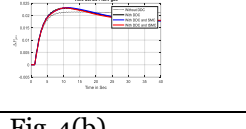
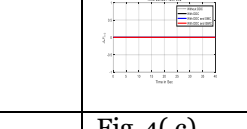
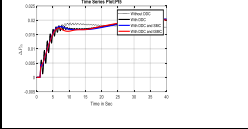
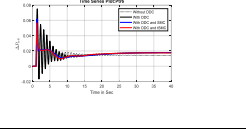
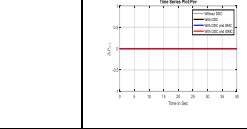
$$\Delta P_{tie13} = \{ \text{Demand of Discos in area -3 from Gencos in area -1} \} - \{ \text{Demand of Discos in area-1 from Gencos in area -3} \}$$

$$\Delta P_{tie13} = [gpf_{15}\Delta P_{L5} + gpf_{16}\Delta P_{L6} + gpf_{25}\Delta P_{L5} + gpf_{26}\Delta P_{L6}] - [gpf_{51}\Delta P_{L1} + gpf_{52}\Delta P_{L2} + gpf_{61}\Delta P_{L1} + gpf_{62}\Delta P_{L2}] \quad (26)$$

$$\Delta P_{tie13} = [0.5 \times 0.1 + 0 \times 0.1 + 0 \times 0.1 + 0 \times 0.1] - [0 \times 0.1 + 0.25 \times 0.1 + 0 \times 0.1 + 0 \times 0.1] = 0.25 \text{ puMW}$$

In three CA power system achieved zero tie-line power deviation as illustrated in Fig- 2(a), (b), and (c). These figures clearly demonstrate that the settling time of $\Delta P_{tie1,3}$ for the PI, PI with DDC, and SMC controllers are longer, 68.761, 42.006 & 40.101sec respectively, compared to TSMC. The complete transient dynamic response parameters for all four controllers are presented in Table-I. It is evident from Table-I that the TSMC controller enhances the settling times of ΔF_1 , ΔF_2 , ΔF_3 , ΔP_{tie12} , ΔP_{tie23} , and ΔP_{tie13} by 5.7483%, 5.1790%, 1.6404%, 8.9650%, 10.3361%, and 11.8960%, respectively, compared to the sliding mode controller with DDC. Generator output power responses are depicted in Fig-3,4 & 5.



| | | |
|------------------------------------------------------------------------------------------------------------------|-------------------------------------------------------------------------------------|--------------------------------------------------------------------------------------|
|  |  |  |
| Fig-2(a) | Fig-2(b) | Fig-2(c) |
| CA- 1,2&3 Tie-line power deviations in bilateral Open market transaction scenario depicted in Fig-2 (a),(b),(c). | | |
|  |  |  |
| Fig-3(a) | Fig-3(b) | Fig-3(c) |
| Fig- 3.(a),(b),(c) of GENCOs mechanical power output response in bilateral transaction scenario in CA-1 | | |
|  |  |  |
| Fig-4(a) | Fig-4(b) | Fig-4(c) |
| Fig-4.(a),(b),(c) of GENCOs mechanical power output response in bilateral transaction scenario in CA-2 | | |
|  |  |  |
| Fig-5(a) | Fig-5(b) | Fig-5(c) |
| Fig-5.(a),(b),(c) of GENCOs mechanical power output response in bilateral transaction scenario in CA-3 | | |

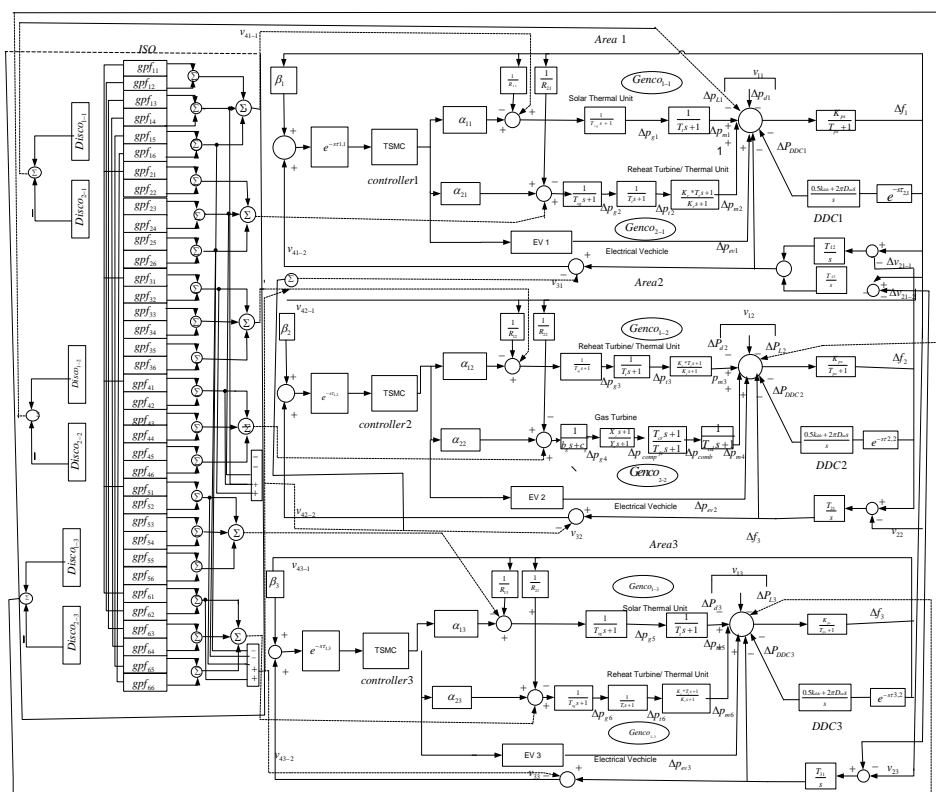


Fig-4. Modified Three-area power system in a deregulated environment

| Controllers | Parameters | Settling time (sec) | Rise time (sec) | Peak time (sec) | Peak overshoot (%) | Undershoot (%) |
|---------------|------------------|---------------------|-----------------|-----------------|--------------------|----------------|
| PI | ΔF_1 | 38.785 | 0.192 | 1.59657 | 7.26395% | 2.76335% |
| | ΔF_2 | 39.491 | 0.17694 | 1.54219 | 6.55317% | 1.87796% |
| | ΔF_3 | 43.652 | 0.2139 | 1.59657 | 5.68164% | 1.48585% |
| | ΔP_{e12} | 44.324 | 0.23403 | 4.04 | 0.93460% | 0.29079% |
| | ΔP_{e23} | 60.898 | 3.28641 | 4.47856 | 0.47132% | 0.19272% |
| | ΔP_{e13} | 68.761 | 2.72217 | 4.0426 | 0.17214% | 10.33710% |
| PI with DDC | ΔF_1 | 27.674 | 0.16836 | 1.5616 | 6.96880% | 2.68152% |
| | ΔF_2 | 25.968 | 0.16828 | 1.515 | 6.33475% | 1.52160% |
| | ΔF_3 | 24.678 | 0.18605 | 1.4616 | 5.31874% | 1.43095% |
| | ΔP_{e12} | 32.618 | 0.170708 | 1.53482 | 0.40911% | 0.13828% |
| | ΔP_{e23} | 43.49 | 1.7711 | 3.70958 | 0.35047% | 0.17134% |
| | ΔP_{e13} | 42.006 | 2.5786 | 3.8527 | 0.15688% | 1.71199% |
| SMC with DDC | ΔF_1 | 20.411 | 0.12921 | 1.4553 | 3.08683% | 2.07717% |
| | ΔF_2 | 21.312 | 0.13255 | 1.42613 | 3.36484% | 1.54055% |
| | ΔF_3 | 21.342 | 0.16841 | 1.515 | 2.83570% | 1.16543% |
| | ΔP_{e12} | 47.975 | 0.23501 | 1.49905 | 0.22571% | 0.35767% |
| | ΔP_{e23} | 42.118 | 2.021 | 4.747 | 1.84229% | 0.04011% |
| | ΔP_{e13} | 40.101 | 2.626 | 4.646 | 0.24838% | 1.50149% |
| TSMC with DDC | ΔF_1 | 19.2377 | 0.10756 | 1.3631 | 1.72950% | 1.73651% |
| | ΔF_2 | 20.20825 | 0.11225 | 1.36958 | 2.06906% | 1.30009% |
| | ΔF_3 | 20.99189 | 0.12726 | 1.14789 | 1.92148% | 0.98016% |
| | ΔP_{e12} | 43.67404 | 0.21623 | 1.18524 | 0.18169% | 0.30278% |
| | ΔP_{e23} | 37.7646 | 1.8977 | 4.374 | 1.60540% | 0.02736% |
| | ΔP_{e13} | 35.33058 | 1.99014 | 4.084 | 0.18267% | 1.32102% |

Table 1. Time Domain Specifications for bilateral based contract case with various controllers

APPENDIX

Parameters values and System Model

Area 1

$T_{ig}=0.08$ s, $T_{i1}=0.3$ s, $K_r=0.5$, $T_r=10$ s, $K_{ps}=120$, $T_{ps}=20$ s, $D=0.015$, $EER=3.75$, $m=0.15$, $c_p=0.5$, $a_{11}=0.5$, $\alpha_{21}=0.5$, $\beta_1=0.4250$, $T_{12}=0.0389$, $R_{11}=2.4$, $R_{21}=2.5$

Area 2

$T_{ig}=0.08$ s, $T_{i1}=0.3$ s, $K_r=0.5$, $T_r=10$ s, $b_g=0.5$, $c_g=1$, $X_c=0.6$, $Y_c=1$, $T_{cd}=0.015$, $T_{fg}=0.23$ s, $T_{cd}=0.2$ s, $K_{ps}=120$, $T_{ps}=20$ s, $D=0.015$, $EER=3.75$, $m=0.15$, $c_p=0.5$, $a_{12}=0.5$, $\alpha_{22}=0.5$, $\beta_2=0.3966$, $T_{23}=0$, $R_{12}=2.5$, $R_{22}=2.7$

Area 3

$T_{ig}=0.08$ s, $T_{i1}=0.3$ s, $K_r=0.5$, $T_r=10$ s, $K_{ps}=120$, $T_{ps}=20$ s, $D=0.015$, $EER=3.75$, $m=0.15$, $c_p=1.01$, $\alpha_{13}=0.5$, $\alpha_{23}=0.5$, $\beta_3=0.3522$, $T_{13}=0.0337$, $R_{13}=2.8$, $R_{23}=0.4$

CONCLUSION

A robust TSMC-DDC was designed for a smart, three-area deregulated renewable energy and EV integrated power system. The TSMC-DDC performance investigated on the three-area open market restructured power system by considering the effect of communication delay in bilateral transaction case. The dominance of the designed TSMC-DDC is demonstrated in terms of the dynamic time domain parameters such as settling time and overshoot, which are compared to SMC-DDC and PI-DDC. The simulation results reveal that the TSMC with DDC controller has low settling time, peak time, undershoot, and overshoot in bilateral contract scenario against PI and SMC with DDC. Furthermore, simulation results disclose that the TSMC provides robustness against parameter uncertainties and changes in load with time delays. The TSMC-DDC damps out frequency deviation and tie line power deviation effectively in contrast to SMC-DDC, PI-DDC, and without DDC.

REFERENCES

- [1] Kumar, P., and Kothari, D. P., "Recent philosophies of automatic generation control strategies in power system," *IEEE Trans. Power Syst.*, Vol. 20, No. 1, pp. 346–357, February 2005.
- [2] Kothari, Dwarkadas Pralhaddas, and I. J. Nagrath. *Modern power system analysis*. Tata McGraw-Hill Publishing Company, 2003.
- [3] Saadat, Hadi. *Power system analysis*. Vol. 2. McGraw-hill, 1999.
- [4] Kundur P. *Power system stability and control*. New York: McGraw-Hill; 1994.
- [5] Bevrani, H., *Robust Power System Frequency Control*, Berlin: Springer, 2009.
- [6] Pourmousavi, S. A., & Nehrir, M. H. (2014). Introducing dynamic demand response in the LFC model. *IEEE Transactions on Power Systems*, 29(4), 1562-1572.
- [7] Jay, D., & Swarup, K. S. (2016, March). Demand Response based Automatic Generation Control in smart-grid deregulated market. In *2016 IEEE 6th International Conference on Power Systems (ICPS)* (pp. 1-8). IEEE.
- [8] Khan, K. A., Quamar, M. M., Al-Qahtani, F. H., Asif, M., Alqahtani, M., & Khalid, M. (2023). Smart grid infrastructure and renewable energy deployment: A conceptual review of Saudi Arabia. *Energy Strategy Reviews*, 50, 101247.
- [9] D. Jay and K. S. Swarup, "Frequency restoration using Dynamic Demand Control under Smart Grid Environment," *ISGT2011-India*, Kollam, India, 2011, pp. 311-315, doi: 10.1109/ISET-India.2011.6145408
- [10] Q. Zhu, W. Yao, L. Jiang, C. Luo and Q. H. Wu, "Load frequency control with dynamic demand control for deregulated power system," *2014 IEEE PES General Meeting | Conference & Exposition*, National Harbor, MD, USA, 2014, pp. 1-5, doi: 10.1109/PESGM.2014.6939313.
- [11] P. Babahajiani, Q. Shafiee and H. Bevrani, "Intelligent Demand Response Contribution in Frequency Control of Multi-Area Power Systems," in *IEEE Transactions on Smart Grid*, vol. 9, no. 2, pp. 1282-1291, March 2018, doi: 10.1109/TSG.2016.2582804

- [12] Y. -Q. Bao, Y. Li, B. Wang, M. Hu and P. Chen, "Demand response for frequency control of multi-area power system," in *Journal of Modern Power Systems and Clean Energy*, vol. 5, no. 1, pp. 20-29, January 2017, doi: 10.1007/s40565-016-0260-1
- [13] Zhu, Qi, Lin Jiang, Wei Yao, Chuan-Ke Zhang, and Cheng Luo. 2016. "Robust Load Frequency Control with Dynamic Demand Response for Deregulated Power Systems Considering Communication Delays." *Electric Power Components and Systems* 45 (1): 75–87. doi:10.1080/15325008.2016.1233300.
- [14] Bharti, K., Singh, V. P., & Singh, S. P. (2020). Impact of Intelligent Demand Response for Load Frequency Control in Smart Grid Perspective. *IETE Journal of Research*, 68(4), 2433–2444. <https://doi.org/10.1080/03772063.2019.1709570>.
- [15] Zhang, C. K., Jiang, L., Wu, Q. H., He, Y., & Wu, M. (2013). Delay-dependent robust load frequency control for time delay power systems. *IEEE Transactions on Power Systems*, 28(3), 2192-2201.
- [16] Ramakrishnan, K., & Ray, G. (2015). Improved results on delay-dependent stability of LFC systems with multiple time-delays. *Journal of Control, Automation and Electrical Systems*, 26, 235-240.
- [17] Webborn, E., & MacKay, R. S. (2017). A stability analysis of thermostatically controlled loads for power system frequency control. *Complexity*, 2017(1), 5031505.
- [18] Hote, Y. V., & Jain, S. (2018). PID controller design for load frequency control: Past, present and future challenges. *IFAC-Papers Online*, 51(4), 604-609.
- [19] Kumar, K. V., Kumar, T. A., & Ganesh, V. (2016, November). Chattering free sliding mode controller for load frequency control of multi area power system in deregulated environment. In *2016 IEEE 7th power India international conference (PIICON)* (pp. 1-6). IEEE.
- [20] Pourmousavi, S. Ali, et al. "LFC model for multi-area power systems considering dynamic demand response." *2016 IEEE/PES Transmission and Distribution Conference and Exposition (T&D)*. IEEE, 2016.
- [21] Shayeghi, Hossein et al. "multi-stage fuzzy PID power system automatic generation controller in deregulated environments." *Energy Conversion and Management* 47 (2006): 2829-2845.
- [22] S. A. Pourmousavi, M. Behrangrad, M. H. Nehrir and A. J. Ardakani, "LFC model for multi-area power systems considering dynamic demand response," *2016 IEEE/PES Transmission and Distribution Conference and Exposition (T&D)*, Dallas, TX, USA, 2016, pp. 1-5, doi: 10.1109/TDC.2016.7519908.
- [23]. Wu, Y., Yu, X., & Man, Z. (1998). Terminal sliding mode control design for uncertain dynamic systems. *Systems & Control Letters*, 34(5), 281-287.
- [24] Yu, X., Feng, Y., & Man, Z. (2020). Terminal sliding mode control—an overview. *IEEE Open Journal of the Industrial Electronics Society*, 2, 36-52.
- [25] Feng, Yong, Xinghuo Yu, and Fengling Han. "On nonsingular terminal sliding-mode control of nonlinear systems." *Automatica* 49.6 (2013): 1715-1722.
- [26] Sina, Alireza, and Damanjeet Kaur. "An optimal controller for load frequency control in multi-area deregulated power system." *Journal of Electrical Systems* 15.1 (2019): 142-158.
- [27] Sahoo, Abhilipsa, Prakash Kumar Hota, and B. Mohanty. "Automatic Generation Control in Deregulated Power Market Using Sunflower Optimization Algorithm." *Innovation in Electrical Power Engineering, Communication, and Computing Technology: Proceedings of IEPCCT 2019*. Springer Singapore, 2020.